Soft Matter

View Online
Dynamic Article Links

Cite this: *Soft Matter*, 2011, **7**, 6637

www.rsc.org/softmatter

PAPER

Mechanomutable and reversibly swellable polyelectrolyte multilayer thin films controlled by electrochemically induced pH gradients

Daniel J. Schmidt, Younjin Min and Paula T. Hammond*

Received 22nd March 2011, Accepted 23rd May 2011
DOI: 10.1039/c1sm05489a

We present a new strategy to electrochemically control the swelling state and mechanical properties of a polyelectrolyte multilayer thin film. While a number of pH-responsive polymer films and hydrogels have been developed, biological systems typically will not tolerate substantial deviations in pH. Therefore, to apply such pH-responsive systems for biomedical or other sensitive applications, we developed an electrochemical approach to alter local pH, while maintaining a constant, mild, bulk pH. The polymer film investigated in this work comprises polyallylamine hydrochloride (PAH) and sulfonated polystyrene (SPS) assembled at high pH (>9.0), which is known to exhibit a large pH-induced swelling transition; however, relatively extreme bulk pH values (pH < 4 to swell, and pH > 10.5 to deswell) are required to manipulate the film. Here, we apply negative electric potentials to gold electrodes coated with the film; the potential induces the reduction of dissolved oxygen, which generates hydroxide ions at the electrode surface and raises the local pH. The *in situ* swelling state and mechanical properties of the film have been probed with a number of techniques. Overall, we have attained reversible 300% volume changes in the polymer thin films, and have reversibly altered the mechanical properties over an order of magnitude (shear modulus between 1.9 MPa and 230 kPa, loss modulus between 620 kPa and 92 kPa, and effective indentation modulus between 19.2 MPa and 3.16 MPa). We maintain that electrochemical control over local pH is a promising strategy to manipulate pH-responsive polymer systems for biomedical and other applications.

Introduction

Stimuli-responsive materials hold great promise for a number of applications including, for example, drug delivery, mechanical actuation/artificial muscles, filtering and separations, flow control in microfluidic devices, and the control of cellular behavior on surfaces.[1–6] While a wide range of external stimuli are available including changes in pH, ionic strength, temperature, and humidity, as well as exposure to light and application of electric and magnetic fields, not all of these stimuli are conveniently applied or amenable to sensitive biological systems. Electric or electrochemical stimuli are especially advantageous since they can be applied rapidly, reversibly, locally, and under relatively mild conditions. Furthermore, such stimuli can be integrated with silicon-based microelectronics and applied remotely using wireless technology. In light of these benefits, the field of organic bioelectronics has grown rapidly in recent years.[7]

Electro-responsive layer-by-layer (LbL) polymer films in particular represent a versatile class of stimuli-responsive materials. Introduced in the 1990s, LbL assembly is a surface-mediated self-assembly process that involves the alternating adsorption of materials with complementary functional groups.[8,9] These materials are typically synthetic or naturally occurring polyelectrolytes, but the films may also incorporate multifunctional nanoparticles and small molecules. The broad array of potentially incorporated functional and responsive materials has led to widespread applications of these films as controlled release coatings, sensors, perm-selective membranes, electrochromic films, and ultra strong composites, among many other applications.[10–12] Further, as reviewed by Sukhishvili, LbL films can be engineered to respond to a number of external stimuli.[13] Our group and others have specifically utilized an electrical stimulus to trigger dissolution[14–18] of LbL films for applications in drug delivery or to trigger swelling and mechanical changes[19–21] in LbL films for a number of potential applications. Zahn *et al.* recently reviewed the growing field of electrochemically controlled swelling of polyelectrolyte multilayers.[22]

Two predominant strategies are evident in the literature for engineering electro-responsive LbL films. The first strategy involves the incorporation of transition metal complexes[19,20] or nanoparticles[18,21] that exhibit multiple stable oxidation states. Upon application of an oxidizing or reducing electric potential, excess charge may then be introduced into the film through

Massachusetts Institute of Technology, Department of Chemical Engineering, 77 Massachusetts Ave., Cambridge, MA, 02139, USA. E-mail: hammond@mit.edu; Fax: +617-258-7577; Tel: +617-258-8992

switching of the oxidation state at the metal centers. This excess charge will induce an influx of ions to maintain electroneutrality along with electroosmotic influx of water. Our group showed that polymer nanocomposite films containing Prussian Blue (PB) nanoparticles and polyethyleneimine swell to 2–10% of their initial hydrated thickness and decrease their Young's elastic modulus by 50% when the PB is electrochemically reduced.[21] Similarly, Grieshaber *et al.* achieved 5–10% swelling through the oxidation of ferricyanide ions incorporated into poly(L-glutamic acid)/poly(allylamine hydrochloride) films.[20] Finally, Forzani *et al.* demonstrated a roughly 10% degree of swelling by electrochemical oxidation of Os(II) to Os(III) in LbL films comprising osmium complex-derivatized polyallylamine and glucose oxidase.[19] Besides film swelling, in which the film stability is not compromised, film dissolution may be achieved when cohesive ionic bonds in the film are directly broken[18,23] or otherwise disrupted by motion of ions.[17] The second strategy for designing electro-responsive LbL films involves the application of electric potentials sufficient to induce local pH gradients; this strategy is applicable to films that are themselves not electrically conducting, but rather are pH-responsive. An oxidizing potential may be applied to lower the local pH *via* the oxidative hydrolysis of water,[14–16] or a reducing potential may be applied to raise the local pH *via* reduction of dissolved oxygen or reductive hydrolysis of water.[24] Previously, this strategy has only been used to induce the dissolution of LbL films,[24] as well as the dissolution of hydrogen-bonded hydrogels[25] and the "opening" and "closing" of an electrode interface modified by a polyelectrolyte brush.[26,27]

In this work, utilizing the second strategy mentioned above, we report on an electrochemically controlled swelling/deswelling and mechanical transition of much greater magnitude than has been reported for other electroresponsive LbL films, and within the range of mechanical stiffness relevant to cellular interactions. The films comprise polyallylamine hydrochloride (PAH) and sulfonated polystyrene (SPS) assembled at pH 9.3, and will be denoted as $(PAH/SPS)_n$ where n is the number of deposited bilayers. As previously reported by the Rubner group, these films exhibit a pH-switchable, discontinuous swelling/deswelling transition with a large hysteresis loop.[28–30] When exposed to a pH ≤ 4, the films swell to 400–800% of their initial thickness; when exposed to pH ≥ 10.5, the films deswell to their original thickness. The film swelling state is dictated by the degree of ionization of the PAH. Here, instead of changing *bulk* pH, we control the film swelling state by manipulating only the *local* pH. In solutions with bulk pH in the range of 3 to 4, we apply electric potentials that reduce dissolved oxygen by Reactions 1 and 2 below. At more negative potentials, water can be reduced by Reaction 3 below.

$$O_2 + 2\,H_2O + 2\,e^- \rightarrow H_2O_2 + 2\,OH^- \quad (1)$$

$$O_2 + 2\,H_2O + 4\,e^- \rightarrow 4\,OH^- \quad (2)$$

$$2\,H_2O + 2\,e^- \rightarrow H_2 + 2\,OH^- \quad (3)$$

The generation of hydroxide ions raises the pH in the vicinity of the electrode, allowing for film deswelling (Scheme 1). Switching the voltage off causes the pH gradient to dissipate and the film to reswell. We study the influence of different variables

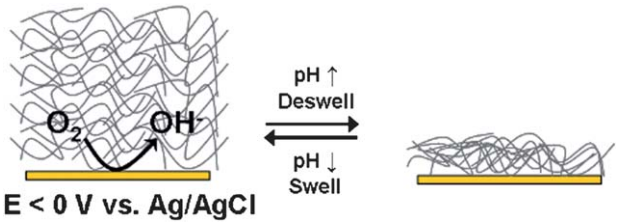

Scheme 1 Schematic of an electrochemically induced deswelling of a polymer thin film through an increase in local pH.

(film thickness, magnitude of the applied voltage, and bulk pH) on the magnitude, kinetics, and reversibility of the electrochemically controlled swelling/deswelling transition utilizing *in situ* electrochemical spectroscopic ellipsometry. To probe film mechanical properties, we utilize an electrochemical quartz crystal microbalance with dissipation monitoring (EQCM-D) and AFM nanoindentation.

Results and discussion

Film assembly and swelling

The thickness of $(PAH/SPS)_n$ films assembled at pH 9.3/9.3 on Au-coated Si was measured with spectroscopic ellipsometry. Fig. 1 shows the film thickness as a function of number of deposited bilayers, n, for films in the dry state, immersed in DI water for 5 min, and immersed in a pH 4 electrolyte solution (3.6 mM NaCl) for 15 min. These films exhibit linear growth, meaning that thickness increases linearly with n, with a thickness per bilayer of roughly 6–8 nm based on dry thickness. Using atomic force microscopy (AFM), the root mean squared (RMS) surface roughness was determined to be approximately 1.7 nm, 2.3, nm, 3.3 nm, and 4.0 nm for the n = 3.5, 5.5, 7.5, and 9.5 films, respectively, in the dry state. Furthermore, as determined by AFM (data not shown), the films of all thicknesses studied here are homogenous and conformally coat the underlying substrate, in agreement with Guillaume-Gentil *et al.*[31] who studied the same material system on gold substrates.

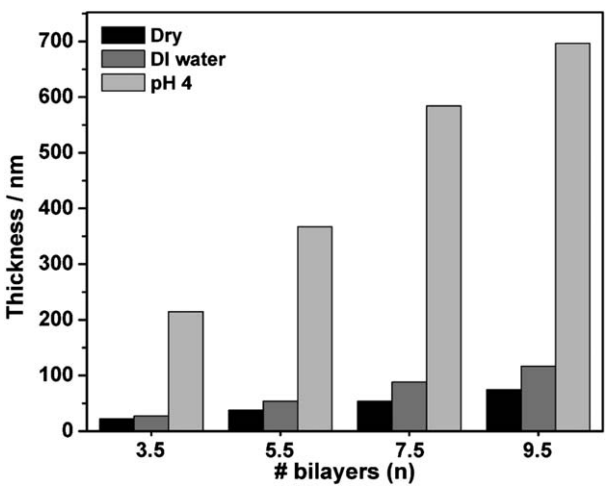

Fig. 1 Thickness of $(PAH/SPS)_n$ films in the dry state, immersed in DI water for 5 min, and immersed in pH 4 water for 15 min, as determined with spectroscopic ellipsometry.

The swelling behavior of the films is summarized in Table 1. In DI water (pH 5.5–6.0) the films swell moderately by roughly 24–63% of dry thickness, reaching a plateau swollen thickness within 1 min. When exposed to pH ≤ 4, the films swell dramatically to 833–983% of their dry thickness and 500–685% of their hydrated thickness in DI water within 15 min. These swelling results are in accordance with previous reports from the Rubner group, who showed that pH ~4 is the onset swelling pH corresponding roughly to the pK_a of the PAH in the as-assembled film.[28,29] Note that the pK_a is shifted to more acidic values compared to that of free PAH (~8.5) in solution due to the hydrophobic microenvironment in the film.[28,32] At the effective film pK_a, the degree of ionization of PAH changes from about 70% to above 95% as measured *via* FTIR by the Rubner group.[29] In response to the excess positive charges introduced in the film as well as the local acidic environment, counterions (*e.g.* OH^-, Cl^-), to maintain electroneutrality, and water, due to osmotic pressure, enter the film and disrupt hydrophobic interactions resulting in a dramatic swelling transition. With the film in the swollen state, the pK_a of the PAH is shifted back to higher pH values;[28,29] at a pH of 10.5, the film deswells back to its original thickness, forming a large hysteresis loop.

Electrochemically triggered deswelling

While it is well established that the swelling state of PAH/SPS films may be controlled with *bulk* pH, here we demonstrate control over the swelling state at a constant bulk pH using an electrochemically induced *local* pH change. A three-electrode electrochemical cell was set up on the stage of a spectroscopic ellipsometer inside a quartz cell (see Experimental section), which allowed simultaneous application of an electric potential to the film-coated electrode plus measurement of film thickness. As shown in a previous publication from our group, application of voltages in the range −0.25 V to −1.00 V (*vs.* Ag/AgCl (3M NaCl)) to gold substrates results in the reduction of dissolved oxygen at the electrode surface.[24] That reaction generates hydroxide ions, which raise the local/interfacial pH near the electrode surface.[33] As an initial proof of concept, we immersed a $(PAH/SPS)_{5.5}$ film in a pH 4 electrolyte solution, such that the film underwent a swelling transition from ~54 nm thick in DI water to ~390 nm thick in the pH 4 solution. When a potential of −0.50 V was applied, the film underwent a deswelling transition to a thickness of 49 nm, near its original thickness in DI water, within 1 min (Fig. 2A). When the potential was turned off and the open circuit potential was restored (~0.20 V), the film gradually reswelled to ~195 nm (Fig. 2A) as the local pH gradient was "erased" by diffusion of the hydroxide ions into the bulk solution. Multiple swell/deswell cycles were performed to assess the reversibility of the transition (Fig. 2B). It is apparent that after the first deswelling transition, the film does not reswell to its original thickness. Rather, it only attains approximately 50% of its original thickness. Subsequent swell/deswell cycles exhibit relatively reversible behavior with only a slight decrease in film thickness over time. Similar trends were observed for all films studied regardless of film thickness, bulk pH, and the applied potential. The decrease in swellability after the first swell cycle is in contrast to observations made by Itano *et al.*,[29] who observed a slight increase in swelling after the first cycle for the same thin film system. To resolve this discrepancy, a series of control experiments were carried out to identify whether the method of raising pH (electrochemically or through bulk pH changes) or the choice of substrate (Au-coated Si *versus* bare Si) was responsible for the irreversibility. The control experiments

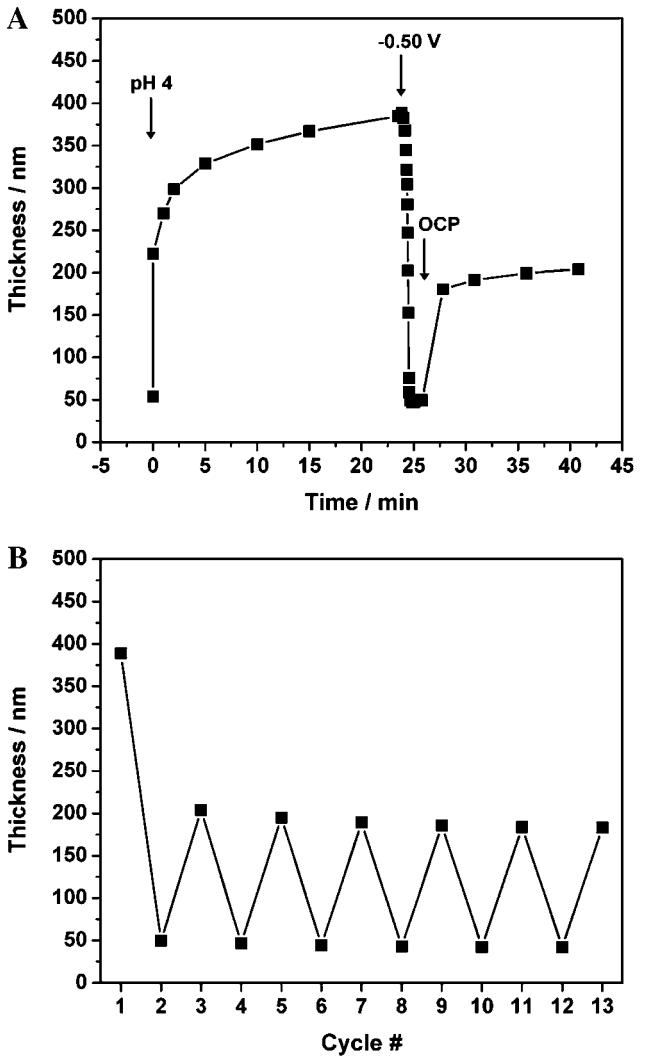

Fig. 2 (A) Thickness of $(PAH/SPS)_{5.5}$ swollen at pH 4, deswollen at −0.50 V, and reswollen at the open circuit potential (OCP). (B) Thickness of $(PAH/SPS)_{5.5}$ after multiple swell (at pH 4) and deswell (−0.50 V) cycles. Odd numbered cycle numbers correspond to the OCP, while even numbered cycles correspond to application of −0.50 V. The thickness values shown were recorded after 10 min at the OCP and 2 min at −0.50 V.

Table 1 Percent swelling (relative to dry thickness) of $(PAH/SPS)_n$ films in DI water and in pH 4 water

n	% Swelling (DI Water)	% Swelling (pH 4 Water)
3.5	24.4	876
5.5	43.5	876
7.5	63.2	983
9.5	56.3	833

revealed (data not shown) that the substrate was the primary source of the discrepancy. The same irreversibility was observed on the Au-coated Si substrates when bulk pH was used to induce film swelling/deswelling. Furthermore, when bulk pH was used to induce film swelling/deswelling on Si substrates, the swelling/deswelling was reversible. While the exact nature of this "substrate effect" is not known, the incomplete reswelling of the film must stem from either permanent densification of the film or loss of some film material following the first swell/deswell cycle. If film densification were occurring, we would expect the films to exhibit higher indices of refraction and greater shear elastic moduli following any densification. We observed, however, that these values are equivalent for films before and after multiple swell/deswell cycles. Therefore, we believe that the films on Au-coated silicon contain some weakly bound material that is lost during the first swell/deswell cycle. Nonetheless, as mentioned earlier and shown in Fig. 2B, excellent reversibility is achieved for subsequent swell/deswell cycles.

Effect of film thickness on deswell kinetics

Since film swelling and deswelling rely on the transport of water into and out of the film, respectively, we expected the swelling/deswelling kinetics to vary with the film thickness. To study this variable, we investigated $(PAH/SPS)_n$ films with $n = 3.5$, 5.5, 7.5, and 9.5. Fig. 3A shows the kinetics of electrically triggered deswelling at an applied potential of −0.50 V at pH 4. Qualitatively, it is clear that thicker films deswell more slowly than thinner films given the greater distance required for the transport of water to reach the same degree of swelling. The half deswelling time ($t_{1/2}$) was quantified based on a Boltzmann sigmoidal fit to the thickness *versus* time data (eqn (4)) where h is the film thickness as a function of time, $h_{deswollen}$ is the film thickness in the deswollen state from the model fit (right, horizontal asymptote), $h_{swollen}$ is the film thickness in the swollen state from the model fit (left, horizontal asymptote), t is time, $t_{1/2}$ is the time at the point of inflection, and t_{width} is the sigmoid width from the model fit. Quantitatively, we found that the square root of the half deswelling time scales linearly with the initial thickness of the film (Fig. 3B). The Boltzmann sigmoid fit all of the deswelling data very well giving R^2 values of at least 0.996. The deswelling time scale was taken as the $t_{1/2}$ value. The square root dependence of deswell time with thickness implies that diffusion may be the rate controlling step for film deswelling. The order of magnitude of the diffusivity of water in the polymer film may then estimated by eqn (5) (for Fickian diffusion), which gives values in the range of 3×10^{-11} to 6×10^{-11} cm^2/s. These values are within the range reported for water diffusivity in hydrophilic polymers[34] and within an order of magnitude of values reported by us for another layer-by-layer film.[35] The reader should note, however, that the poroelasticity of the polymer film, in addition to the diffusivity of the water in the polymer film, may affect the deswell kinetics. In fact, film swelling/deswelling kinetics may also show a square root of time dependence when poroelastic phenomena dominate.[36]

$$h(t) = h_{deswollen} + \frac{h_{swollen} - h_{deswollen}}{1 + \exp\left[\left(t - t_{1/2}\right)\Big/ t_{width}\right]} \quad (4)$$

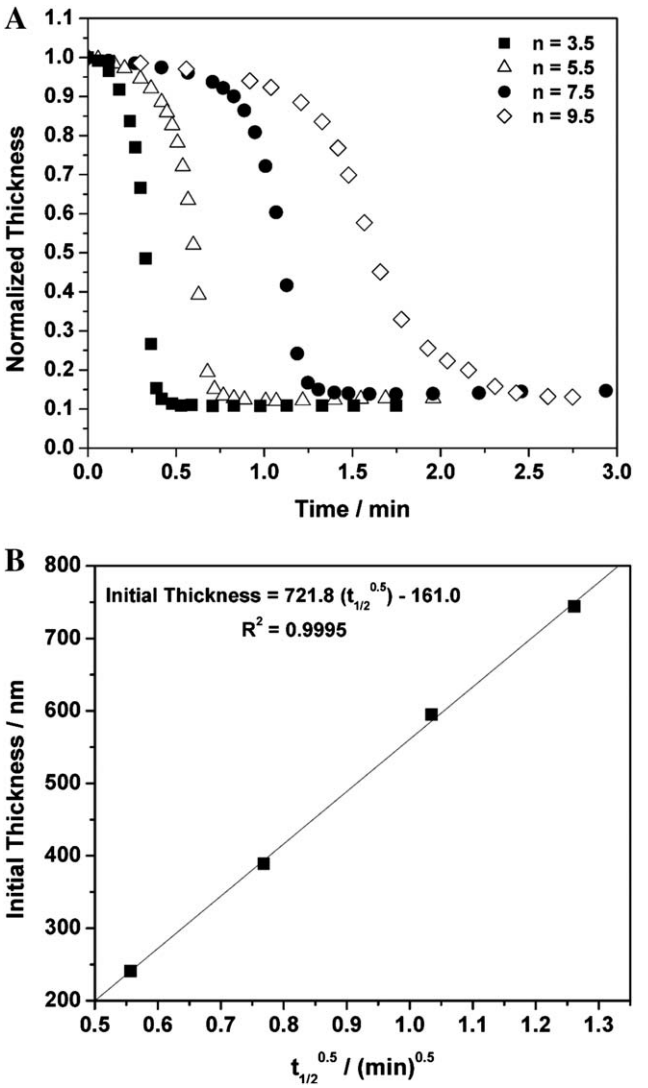

Fig. 3 (A) Thickness of $(PAH/SPS)_n$ at an applied potential of −0.50 V in a pH 4 electrolyte solution. The thickness was normalized to the initial swollen thickness in pH 4, which can be found in Fig. 1. The data shown are for the first deswell cycle. (B) Linear relationship between the initial film thickness and the square root of the deswelling time indicates that diffusion of water out of the film may control the rate of film deswelling.

$$D_{H_2O} \approx \frac{(h_{swollen})^2}{t_{1/2}} \quad (5)$$

Effect of magnitude of applied voltage on deswell kinetics

A key variable to tune the rate of electrochemically induced film deswelling is the magnitude of the applied potential. Since oxygen reduction is a mass-transfer limited process, a current "plateau" (*i.e.*, a constant rate of oxygen reduction) is generally observed in the oxygen reduction potential range.[33] However, as shown by us in a previous publication, application of a more negative potential does modestly increase the rate of oxygen reduction, which speeds up the response of polymer films sensitive to elevated pH.[24] In agreement with these past results, we observe that more negative voltages induce a faster rate of electrochemically triggered deswelling of $(PAH/SPS)_n$ films (Fig. 4). At a bulk pH of 4, for example, the half deswelling time can be

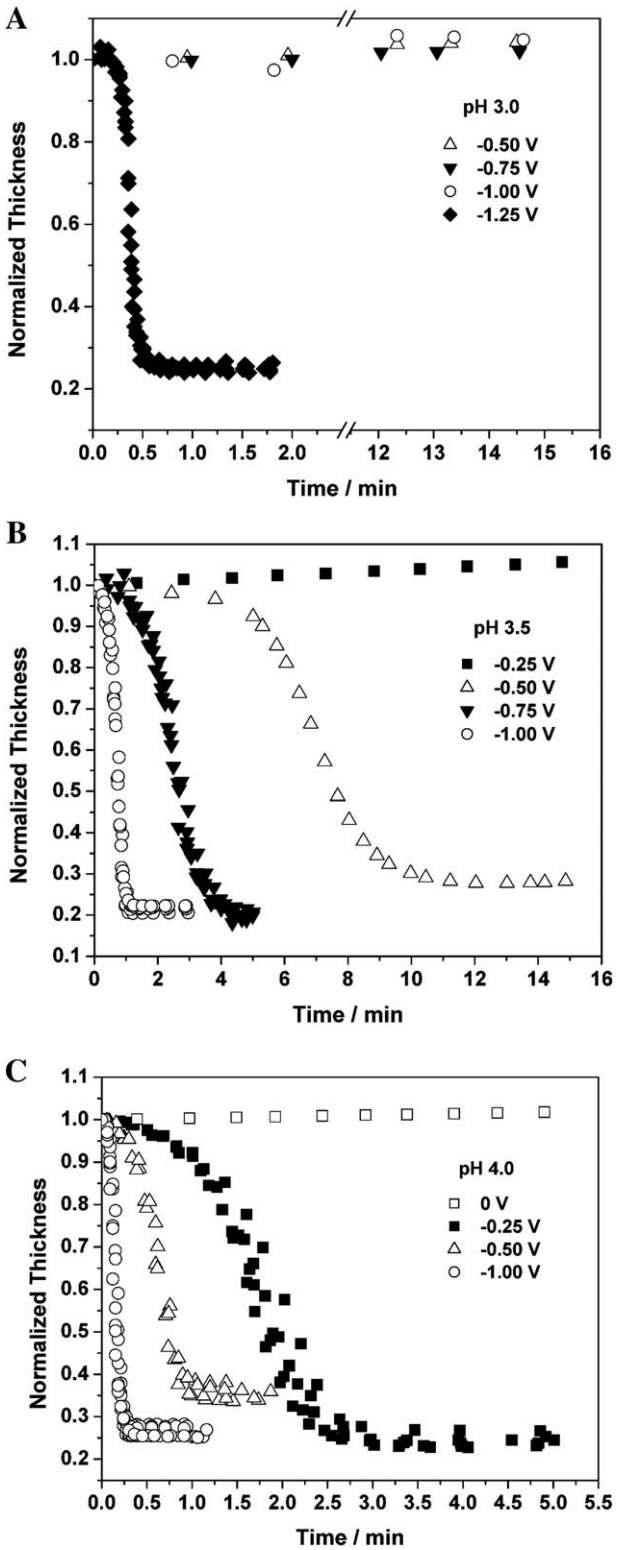

Fig. 4 Normalized thickness *versus* time of $(PAH/SPS)_{5.5}$ films at bulk pH values of (A) 3.0, (B) 3.5, and (C) 4.0. The minimum electric potential required to deswell the film depends strongly on the bulk pH. Thickness is normalized to the swollen film thickness at the open circuit potential after the first swell/deswell cycle. Data for multiple cycles are reported to show reproducibility.

tuned from 9 s at −1.00 V to 1 min 42 s at −0.25 V (Fig. 4C). An applied potential of 0 V does not raise the local pH sufficiently to deswell the film, while a more negative voltage of −1.00 V induces the reduction of water (*i.e.*, decomposition of the solvent) (Reaction 3), which evolves hydrogen gas and also generates hydroxide ions that raise the local pH. Deswelling can be triggered even faster at these more negative voltages (data not shown); however, solvent decomposition and hydrogen evolution may be undesired for an end application.

Effect of bulk pH on deswell kinetics

Above, we described the effect of the magnitude of the applied voltage at a bulk pH of 4, which is roughly the highest pH at which the films exist in a superswollen state.[29] At lower bulk pH values, the same voltage may induce slower deswelling kinetics or may not induce deswelling at all (Fig. 5). In effect, each bulk pH has a different critical voltage that is required to induce film deswelling. The value of the bulk pH evidently affects how high of a local pH may be attained by any given applied potential. In Deslouis *et al.*, the authors neglect the concentration of OH^- ions in the bulk (*i.e.*, the bulk pH) relative to the concentration at the electrode surface for their derivation of the interfacial pH; however, the pH profile (*i.e.*, the concentration of OH- that extends from the electrode interface into the bulk) evidently depends upon the bulk pH, given the results of our experiments.

While reversible swell/deswell cycles controlled by an electrochemical trigger are only possible at pH < 4, it is possible to deswell the film one time under milder pH conditions. As shown by Hiller *et al.*, the PAH/SPS system exhibits a large swelling hysteresis with so-called "molecular memory".[28] If a film is swollen below pH 4 and then transferred to a pH 7.4 solution, it will remain in the swollen state due to the insufficient number of OH- ions to induce the deswelling. Therefore, to demonstrate the electrochemically triggered deswelling phenomenon at milder conditions, we pre-swelled a film at pH < 4, transferred the film to a pH 7.4 solution with equivalent ionic strength (3.6 mM NaCl), and applied −0.25 V (Fig. 6). When the potential is turned off, however, the film will not reswell unless transferred back to a solution with pH < 4 (Fig. 6). While the ability to deswell the film under milder conditions is promising for biomedical applications, there is also an ionic strength dependence on the film swelling state that is not systematically explored in this manuscript. When a film pre-swollen at pH 4 is immersed in a PBS solution (pH 7.4, 0.15 M ionic strength), representative of physiological conditions, the film immediately deswells due to the decrease in the osmotic pressure force. That is, the difference in salt concentration between the film and surrounding solution is no longer sufficient to maintain the film in a superswollen state, thus precluding the electrically triggered deswelling phenomenon at physiologic ionic strengths.

QCM-D

Film growth, swelling, and electrochemically triggered deswelling were also studied using QCM-D. Fig. 7 shows the growth of a $(PAH/SPS)_{5.5}$ film on the QCM crystal. Before swelling, the film was rigid and obeyed the Sauerbrey relationship (eqn (6)), which relates the change in the quartz resonator frequency (Δf) to

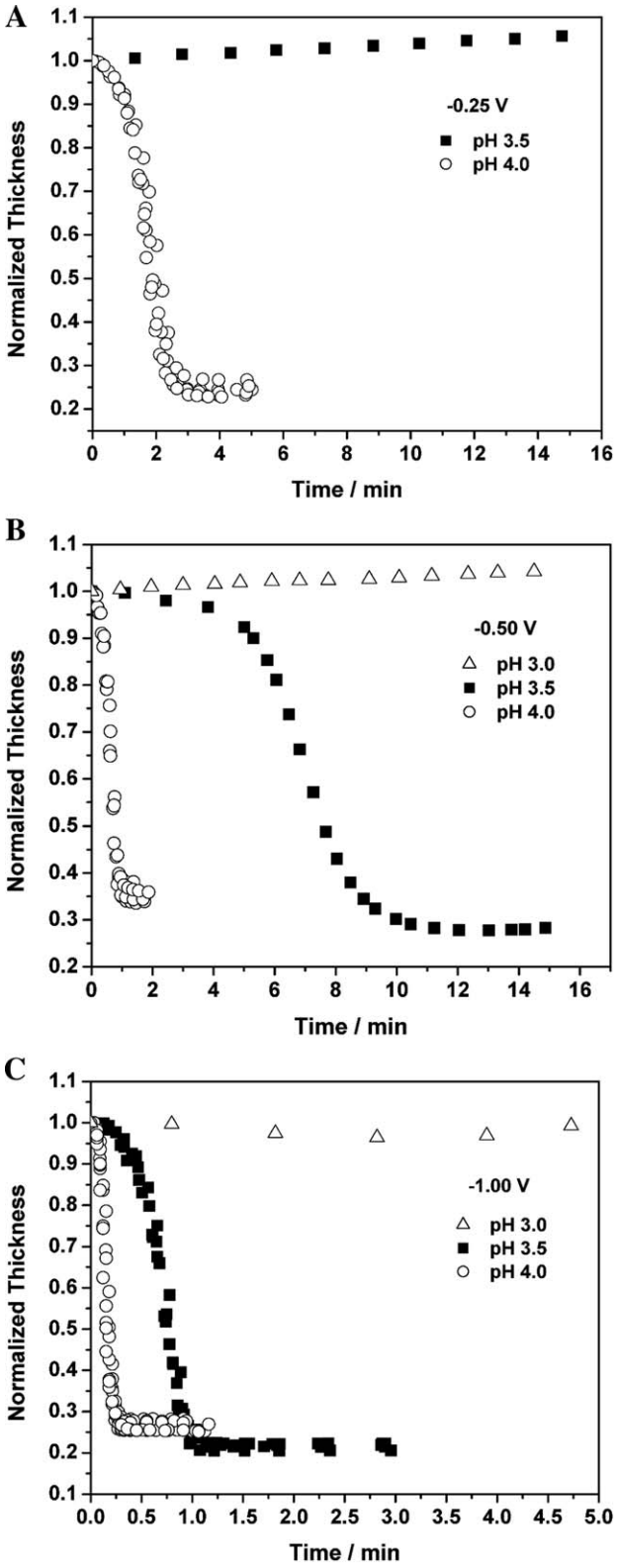

Fig. 5 Normalized thickness *versus* time of $(PAH/SPS)_{5.5}$ films at (A) −0.25 V, (B) −0.50 V, and (C) −1.0 V. Thickness is normalized to the swollen film thickness at the open circuit potential after the first swell/deswell cycle. Data for multiple cycles are reported to show reproducibility.

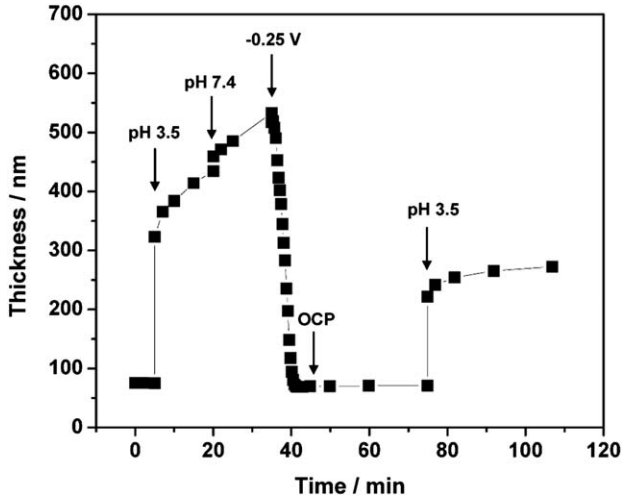

Fig. 6 Thickness of a $(PAH/SPS)_{5.5}$ film initially immersed in DI water, swollen after immersion in pH 3.5 solution, transferred to a pH 7.4 solution, electrochemically deswollen during application of −0.25 V (*vs.* Ag/AgCl (3 M NaCl)), and then reswollen after re-immersion in a pH 3.5 solution. Returning to the open circuit potential (OCP) alone does not cause the film to reswell in the pH 7.4 solution, since that pH is above the critical pH for film swelling.

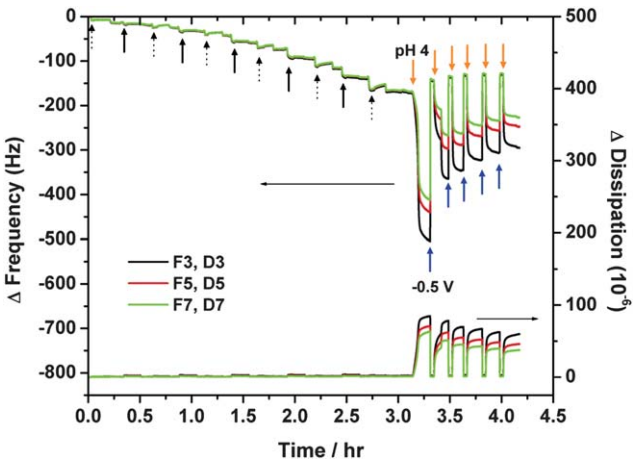

Fig. 7 Change in frequency (F) and dissipation (D) of a QCM crystal during *in situ* build up of a $(PAH/SPS)_{5.5}$ film at pH 9.3/9.3, film swelling at pH 4, electrochemically triggered deswelling at −0.50 V, and reswelling at the open circuit potential (OCP). Dashed black arrows indicate injection of the PAH, while solid black arrows indicate injection of the SPS. Arrows following the film build up phase indicate application of −0.50 V and a return to the OCP. Data are presented for the 3rd (F3, D3), 5th (F5, D5), and 7th (F7, D7) overtones corresponding to resonance frequencies of approximately 15 MHz, 25 MHz, and 35 MHz, respectively.

the change in mass adsorbed to the crystal (Δm), where C (17.7 ng Hz^{-1} cm^{-2}) is a constant related to the physical properties of the quartz and n is the overtone number.

$$\Delta m = -C\left(\Delta f / n\right) \quad (6)$$

The Sauerbrey relationship is valid when all of the frequency overtones overlap.[37] When water with pH = 4 was pumped

into the QCM chamber, the resonance frequencies all dropped substantially, indicating uptake of water into the film. Concomitantly, the dissipation values all rose substantially, indicating that the film became more compliant. The large increase in dissipation and the fact that the different frequency overtones do not overlap when the film is in the swollen state, necessitates the consideration of the viscoelastic properties of the film for accurate determination of film thickness.[37] As described by Voinova *et al.* for thin polymer films in liquid, the polymer film may be considered as a Voigt element to characterize the viscoelasticity of the film.[38] The Voigt element is defined as a spring (representing elastic behavior) and a dashpot (representing viscous behavior) arranged in parallel. Using QTools software we set the variable parameters in the model to be the film thickness, film shear (storage) elastic modulus, and film shear viscosity. The fixed parameters were fluid density (1000 kg m^{-3}), fluid viscosity (1 cP), and film density, which we assumed was equal to that of the density of water. Fig. 8 shows film thickness, shear modulus, and shear viscosity over time for film growth and for multiple swell/deswell cycles achieved by injection of pH 4 water at the open circuit potential and by application of −0.50 V to the gold electrode, respectively. The hydrated film thickness for an n = 5.5 film was determined to be roughly 38 nm with QCM-D. That value is less than the hydrated thickness of films made on gold-coated Si wafers using standard dip coating (~54 nm). As has been demonstrated previously by Cho *et al.* for spin-assembled films, shear forces, which were present during assembly on the QCM crystal, can result in a thinner film.[39] Qualitatively, the QCM-D shows the same film swelling/deswelling behavior as was observed with spectroscopic ellipsometry. Specifically, the films swell substantially at pH 4 and then may be deswelled by application of −0.50 V, which raises the local pH at the electrode surface. Furthermore, QCM shows the same trend with multiple cycles. That is that films reswelled at the OCP do not return to their originally superswollen thickness. Besides determination of film thickness, the Voigt model also provides mechanical information for films in the swollen and deswollen state (Fig. 8B and 8C). From eqn (7) below, one may calculate the shear (storage) modulus (G'), loss modulus (G''), and complex shear modulus ($|G^*|$). Those values for the $(PAH/SPS)_{5.5}$ film are shown in Table 2. Using the electrochemical trigger, we are able to reversibly switch the stiffness of the film over nearly an order of magnitude. The reader should note, however, the limitations in extracting viscoelastic information with a QCM-D. As noted by Vogt *et al.*,[40] the model of Voinova *et al.*[38] assumes viscosity to be independent of frequency and neglects the longitudinal waves from the oscillator. In particular, it is difficult to extract accurate viscoelastic information for films that obey the Sauerbrey relationship and exhibit little to no viscous dissipation. Therefore, the shear storage and loss moduli determined here for films in the deswollen state may be inaccurate. For this reason, we utilized AFM nanoindendation as a complementary technique to measure film mechanical properties.

$$G^* = G' + iG'' = \mu_f + 2\pi f \eta_f \quad (7)$$

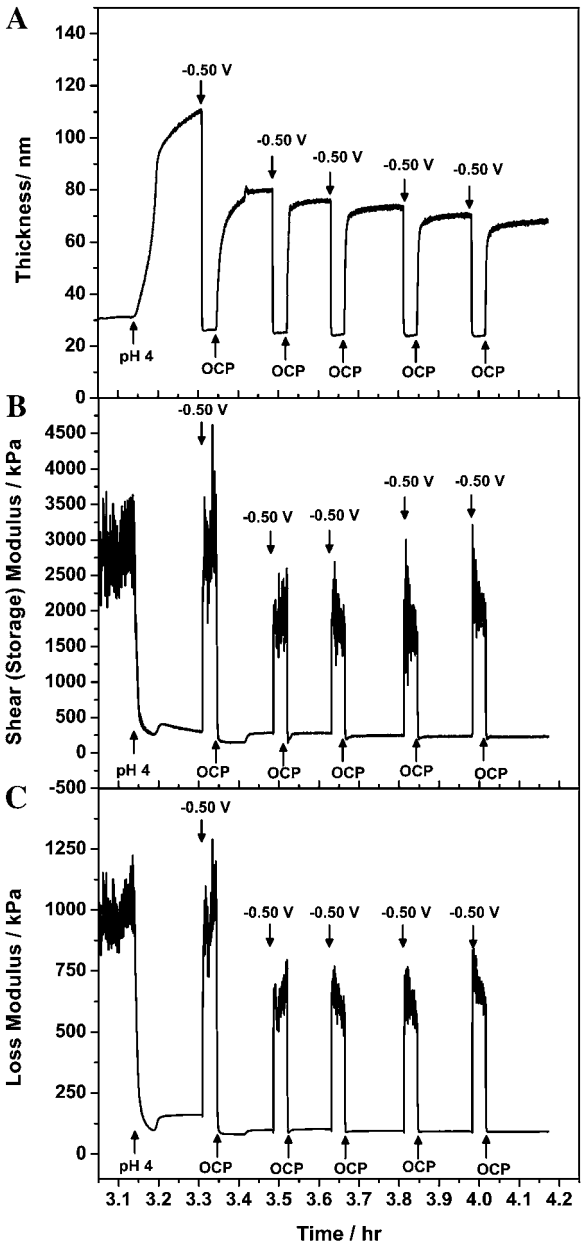

Fig. 8 (A) Thickness of a $(PAH/SPS)_{5.5}$ film swollen upon exposure to pH 4 water, deswollen upon application of −0.50 V, and reswollen at the open circuit potential. (B) Shear (storage) modulus and (C) loss modulus of $(PAH/SPS)_{5.5}$ films during multiple swell (at pH 4, OCP)/deswell (−0.50 V) cycles.

AFM nanoindenation

The mechanical properties of the PAH/SPS films on gold-coated silicon substrates were evaluated by conducting AFM-enabled nanoindentation. Films were initially immersed in DI water (pH 5.5–6.0) with 3.6 mM ionic strength (adjusted with NaCl) to represent the "deswollen state" followed by a pH 3.5 aqueous solution with 3.6 mM ionic strength (adjusted with HCl/NaCl) to induce the superswelling transition. Relatively thicker films ($(PAH/SPS)_{9.5}$ instead of $(PAH/SPS)_{5.5}$) were used to have minimum mechanical contributions from the underlying stiff

Table 2 Mechanical properties of (PAH/SPS) films in the swollen and deswollen states from QCM-D and AFM nanoindentation

	Swollen	Deswollen
Shear (storage) modulus (G')	230 ± 6 kPa	1900 ± 290 kPa
Loss modulus (G'')	92 ± 1 kPa	620 ± 60 kPa
Complex shear modulus ($\|G^*\|$)	250 ± 6 kPa	2000 ± 300 kPa
Effective Indentation Elastic Modulus (E_s)	3.16 ± 0.04 MPa	19.2 ± 0.32 MPa

substrate and therefore to improve the accuracy of the nanoindentation. The inset in Fig. 9 shows sets of applied force (F) *vs.* indentation depth (δ) curves obtained from multiple locations (at least 30) and a corresponding effective indentation elastic modulus, E_s, calculated from eqn (8) and (9) is shown in Fig. 9. The center of the elastic moduli distribution (X_c) was obtained by fitting a Gaussian to histogram plots. Clearly, the film becomes more compliant in the pH 3.5 solution compared to the DI water solution, consistent with an increase in hydration upon film swelling (See Table 1). The $X_{c,\ DI\ water}$ was approximately six times higher than the $X_{c,\ pH\ 3.5}$. The magnitude of this difference (*i.e.*, 6x) between the effective indentation elastic moduli agreed well with the magnitude of the difference between the shear (storage) moduli (G') (*i.e.*, 8x), for the same incubation conditions, obtained by QCM-D. According to Nielsen,[41] when the system is isotropic with a Poisson ratio of 0.5, G' is related to E_s by $G' = E_s/3$; therefore E_s and G′ should exhibit the same trends, as we have observed here. However, we do observe a slight deviation from theory in the experimentally determined

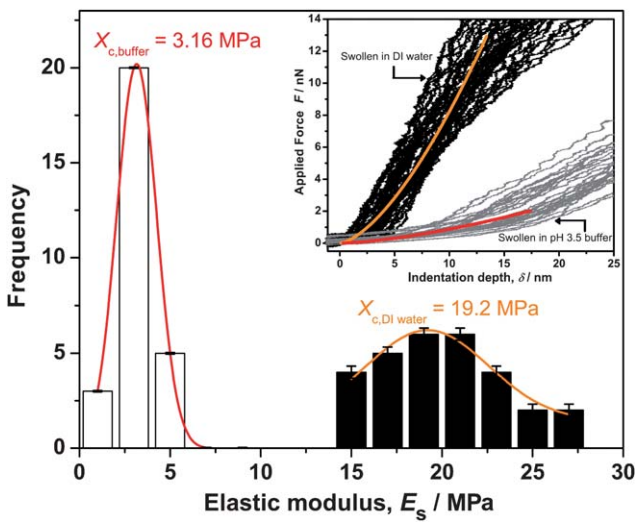

Fig. 9 Measured stiffness of a $(PAH/SPS)_{9.5}$ film swollen in DI water (black columns) and in pH 3.5 water (white columns) by AFM nanoindentation. The inset shows force-depth (F–δ) responses acquired during nanoindentation of the films upon film swelling: immersed in DI water (solid black); immersed in pH 3.5 water (solid grey). The orange and red solid lines shown in the inset are representative fitting curves based on eqn (8) to extract a respective elastic modulus, E_s using eqn (9). The Gaussian fitting to elastic moduli distribution gives respective X_c values, which represents the center of Gaussian distributions.

relationship between E_s and G'. Referring to Table 2, we find that E_s is roughly 13x greater than G' for the film in the swollen state and roughly 10x greater for the film in the deswollen state. This discrepancy with theory might be expected since the nanoindentation is a local measurement with the maximum contact area of 0.001 μm^2 in this study whereas the analysis adopts the model originally developed for macroscopic contact mechanics.[42] Furthermore, E_s often becomes dependent on the film thickness when the film thickness is reduced to the nanoscale,[42] and viscoelastic effects, especially with a high tip approaching velocity,[43] are known to overestimate E_s. Therefore, the stiffness E_s is not intended to be a rigorous measure of the elastic modulus, but is sufficient to provide a qualitative comparison of the effective film stiffness at different pH conditions, allowing for further characterization of the mechanomutable properties of PAH/SPS films.

Experimental

Materials

Poly(allylamine hydrochloride) (PAH) (M_w = 70,000), poly-(4-styrenesulfonic acid) (SPS) (18 wt% in H2O) (M_w = 75,000), hydrogen peroxide (30 wt% solution in water), and ammonium hydroxide (28–30 wt% in water) were purchased from Sigma Aldrich (St. Louis, MO) and used as received. Sodium carbonate and sodium bicarbonate were purchased from Mallinckrodt Chemicals (Phillipsburg, NJ). Hydrochloric acid (1 M solution) and sodium hydroxide (1 M solution) were purchased from VWR International (Radnor, PA). Deionized water (>18.2 MΩ cm resistivity), obtained using a Milli-Q Plus system (Millipore, Bedford, MA), was used to make all solutions. Gold-coated silicon wafers (AU.1000.SL1) consisting of a 1000 Å layer of gold with a 50 Å titanium adhesion layer were purchased from Platypus Technologies (Madison, WI). Gold-coated QCM crystals (QSX 301) consisting of a 1000 Å layer of gold with a 50 Å chromium adhesion layer were purchased from Q-Sense, Inc./Biolin Scientific (Linthicum, MD).

Assembly of PAH/SPS films

Films were assembled on gold-coated silicon wafers or gold-coated AT-cut quartz crystals. Both substrates were cleaned with an RCA cleaning solution (5 : 1 : 1 H_2O:H_2O_2 (30%):NH_3 (25%)) at 75 °C for 5 min, rinsed copiously with deionized water, and dried under a stream of nitrogen gas. Next, each substrate was electrochemically cycled in 0.5 M H_2SO_4 (~20 mL) from 0.2 V to 1.6 V (*vs.* Ag/AgCl (3 M NaCl)) with a Pt wire counter electrode in a three-electrode cell. This cyclic voltammetry (CV) procedure was carried out at scan rate of 1 V s^{-1} for 100 cycles, sufficient to give a stable CV curve. This process activates the gold surface by forming and reducing a gold oxide layer on the surface. Next, the substrates were rinsed thoroughly with DI water and then immersed in a PAH solution for at least 1 h. PAH and SPS solutions were prepared in deionized water at a concentration of 10 mM based on the polymer repeat unit. The pH of the PAH solution was adjusted to pH 9.3 with 1 M NaOH, while the pH of the SPS solution was set to pH 9.3 with a 10 mM carbonate buffer to eliminate pH drift. $(PAH/SPS)_n$ films, where n denotes the number of bilayers, were assembled by dip coating

using an automated Zeiss HMS Series programmable slide stainer. The positively-charged substrates (owing to the layer of PAH) were immersed in an SPS solution for 10 min followed by three separate deionized water rinse baths (adjusted to pH 9.3 with 10 mM carbonate buffer) for a total of three minutes. Next, the substrates were immersed in PAH solution for 10 min followed by the same cascade rinse cycle. This alternating deposition process was repeated until films were assembled with the desired number of bilayers. Gold-coated silicon substrates were used for spectroscopic ellipsometry and AFM nanoindentation, while gold-coated quartz was used for QCM-D.

Spectroscopic ellipsometry

Film thickness was measured both dry and *in situ* at room temperature (25 °C) with spectroscopic ellipsometry using a J.A. Woollam (Lincoln, NE) M-2000 instrument at an incident angle of 70°. *In situ* measurements were conducted through a custom-made quartz cell with 70° windows (Hellma USA, Inc.). Data were modeled using J.A. Woollam WVASE32 software. Since the Au layer on the Au-coated Si substrates is optically thick, only a two-layer model was required to fit the data; specifically, one layer for the gold substrate and one layer for the overlying polymer film. The optical constants of the gold were obtained through a point-by-point fit for refractive index (n) and extinction coefficient (k). The transparent polymer film ($k = 0$) was modeled as a Cauchy layer (two-term only: $n(\lambda) = A_n + B_n/\lambda$) in which the fitted parameters were film thickness, A_n, and B_n over the wavelength range 300–1000 nm. To simultaneously apply a voltage to a film-coated electrode while characterizing the film with spectroscopic ellipsometry, a three-electrode electrochemical cell was set up in the quartz cell with a Ag/AgCl (3 M NaCl) reference electrode (Bioanalytical Systems, Inc.), a Pt coil counter electrode, and a Au-coated Si wafer modified with a $(PAH/SPS)_n$ film as the working electrode. The electrolyte was an NaCl solution with pH 3–4 and a controlled total ionic strength of 3.6 mM (combination of HCl and NaCl). An Auto-Lab PGSTAT100 potentiostat was used for electrochemical measurements. A dynamic scan protocol in the WVASE32 software package with acquisition time of ~10 milliseconds was used to capture the kinetics of the redox-induced swelling process.

Atomic force microscopy (AFM)

AFM imaging of $(PAH/SPS)_n$ films on gold-coated silicon substrates in the dry state was carried out to measure surface roughness and to determine film homogenity on the microscale. A Dimension 3100 Scanning Probe Microscope (Bruker AXS, Madison, WI) was used in tapping mode. A silicon cantilever with nominal probe radius of 8 nm (RTESP, Veeco Metrology Groups, Sunnyvale, CA) was used. Root mean squared roughness values were obtained from AFM images with a size of 5×5 μm^2 using Nanoscope Analysis software (Veeco Metrology Groups, Sunnyvale, CA).

Quartz crystal microbalance with dissipation monitoring (QCM-D)

QCM-D analysis of $(PAH/SPS)_{5.5}$ films on gold-coated quartz was carried out using a Q-Sense E1 system (Q-Sense, Inc./Biolin Scientific (Linthicum, MD)) along with the Electrochemistry Module (QEM 401). The quartz crystals were cleaned as described above, and $(PAH/SPS)_{5.5}$ films were assembled in the QCM chamber by the following procedure. A PAH solution was pumped into the chamber and the polymer was allowed to adsorb for 10 min under static conditions. Next, rinse water was pumped through the chamber for ~3 min at a flow rate of ~1 μL/min. Then an SPS solution was pumped through the chamber, adsorption allowed for 10 min, and rinse water flowed through for ~3 min. The cycle was repeated 5.5 times. Film swelling was then induced by flowing through a pH 4.0 solution (3.6 mM ionic strength adjusted with NaCl). A voltage could then be applied to the film directly in the QCM chamber, which served as a three-electrode electrochemical cell with a Ag/AgCl (3 M NaCl) reference electrode (Cypress Systems/ESA Inc. (Chelmsford, MA)), a built-in Pt counter electrode, and the Au-coated QCM crystal modified with a $(PAH/SPS)_{5.5}$ film as the working electrode. A PG580 potentiostat/galvanostat (Uniscan Instruments, UK) was used for electrochemical measurements. Experiments were carried out at room temperature (25 °C). QTools software (Q-Sense, Inc./Biolin Scientific (Linthicum, MD)) was used to analyze the QCM-D data.

AFM nanoindentation

Mechanical properties of $(PAH/SPS)_{9.5}$ film on gold substrate were acquired in pH 5.5–6.0 solution and in a pH 3.5 solution (both with 3.6 mM ionic strength adjusted with NaCl) at room temperature (25 °C) on a commercial scanning probe microscope (Molecular Force Probe 3D (3DMFP), Asylum Research, Inc., Santa Barbara, CA). Unsharpened silicon nitride cantilevers with nominal probe radius $R_{tip} \approx 20$ nm (MLCT, Veeco Metrology Group, Sunnyvale, CA) were used to obtain the continuous force-displacement responses of the polyelectrolyte multilayers (PEMs) in fluid. Prior to indentation, the actual spring constant k_c of the cantilever was determined experimentally as 0.178 ± 0.006 N m^{-1} using the thermal power spectral density (PSD) method. Nanoindentation was performed at greater than 100 positions at a rate of 500 nm s^{-1} in an acoustic isolation enclosure. Indentation force-displacement responses were analyzed with IGOR Pro software (WaveMetrics, Lake Oswego, OR). A reduced elastic modulus, E_r, of the indented PEMs was then estimated by applying the Hertz contact model (with a finite thickness correction) of the form:

$$F = \frac{16}{9} E_r R_{tip}^{1/2} \delta^{3/2} (1 + 1.133\chi + 1.283\chi^2 + 0.769\chi^3 + 0.0975\chi^4), \quad (8)$$

where F is applied force, R_{tip} is the radius of curvature of the cantilevered probe, and δ is the depth of penetration into the sample surface. χ is defined as $(R_{tip}\delta/h)^{1/2}$ where h is the thickness of the PEM in fluid.[44] The obtained E_r was then used to estimate the effective elastic indentation modulus of LbL films (E_s) based on the relationship:

$$E_r = \frac{E_s}{1 - \nu_s^2} + \frac{E_p}{1 - \nu_p^2}, \quad (9)$$

where E_s, ν_s and E_p, ν_p are the Young's modulus and Poisson's ratio for the sample material (LbL film) and the cantilever probe

material (Si_3N_4), respectively. The Poisson's ratios were assumed to be 0.33 and 0.50 for Si_3N_4 and the films, respectively and E_p was assumed to be equal to 310 GPa.

Conclusions

The electrochemically controlled swelling and mechanical properties of a polyelectrolyte multilayer thin film containing polyallylamine hydrochloride (PAH) and sulfonated polystyrene (SPS) has been described. Application of cathodic electric potentials in the range of −0.25 V to −1.25 V (*vs.* Ag/AgCl (3 M NaCl) to gold electrodes coated with the films induces reduction of dissolved oxygen, which generates hydroxide ions and raises the local (interfacial) pH. Starting in a superswollen state achieved between pH 3 and 4, the films are deswollen when the potential is applied, which raises the local pH to at least 10.5. The increase in pH deprotonates the primary amines of PAH and reforms hydrophobic interactions causing the film to return to a more compact state.[29] Turning off the voltage then "erases" the local pH, allowing it to return to the bulk pH value, which induces reswelling of the thin film. While the first cycle exhibits incomplete reversibility with regard to the reswelling thickness, subsequent cycles are reversible. Overall, we have attained reversible 300% volume changes (*e.g.* between roughly 50 nm and 200 nm for $n = 5.5$ bilayer films) in the polymer thin films, and have reversibly altered the viscoelastic properties over nearly an order of magnitude (shear modulus between 1.9 MPa and 230 kPa, loss modulus between 620 kPa and 92 kPa, and effective indentation elastic modulus between 19.2 MPa and 3.16 MPa). The kinetics of electrically triggered deswelling were found to vary depending upon the film thickness, magnitude of the applied potential, and the bulk pH. Film thickness dictates the timescale for diffusion of water into and out of the film, the magnitude of the potential controls the rate of oxygen reduction, and the bulk pH affects how high of a local pH can be attained at a given potential.

The degree of electrochemically triggered swelling and the magnitude of mechanical changes presented in this work are greater than those reported by us and by others for other polymer thin film systems. We previously reported layer-by-layer systems that undergo 2–10% volume changes and 50% changes in mechanical stiffness,[21] while Grieshaber *et al.* reported 5–10% volume transitions,[20] and Forzani *et al.* reported ~10% volume transitions[19] all utilizing the redox switching of transition metal compounds within the polymer films. A number of other authors have measured up to 30% volume transitions and stiffness changes in the range of 20–300% for different polyaniline and polypyrrole conducting polymer films upon redox cycling.[45–51] These systems tend to undergo smooth, continuous changes driven by motion of ions and changes in polymer backbone stiffness. In contrast, as reported first by Hiller *et al.*, the $(PAH/SPS)_n$ system examined in this work exists in a "frustrated" state and can thereby undergo discontinuous swelling transitions between two energy minima, which are formed by competition between attractive and repulsive interactions.[28]

We maintain that achieving such drastic, discontinuous changes in the swelling and mechanical properties of a surface coating could be particularly useful for such applications as controlling adhesion of proteins or cells on surfaces, drug delivery, and controlling flow in microfluidic systems. The material system presented in this work will only undergo a reversible electrically triggered deswelling transition at a pH < 4, which is not a pH value that is compatible with typical biological systems; however, if the film is first pre-swollen at pH < 4 and then transferred to a milder pH (*e.g.* pH 7–7.4), then it will remain in the swollen state and be capable of electrochemically induced deswelling. In that case, however, the film will not reswell when the electric potential is turned off unless the film is transferred back to pH < 4. Overall, we have introduced a powerful strategy that allows control over classic pH-responsive polymer thin films by only changing the *local* pH. We believe that this strategy could be extrapolated to other material systems and improve the practical applicability of pH-responsive materials for applications in which altering the *bulk* pH is not an option.

Acknowledgements

This work was supported primarily by the MRSEC Program of the National Science Foundation and made use of the MRSEC Shared Experimental Facilities under award number DMR-0819762. We thank the Center for Materials Science and Engineering and the Institute for Soldier Nanotechnologies for access to their facilities. We thank Prof. Krystyn Van Vliet and Adam Zeiger for helpful discussions and assistance with AFM nanoindentation. Y.M. thanks the Institute for Soldier Nanotechnologies for funding.

Notes and references

1 S. K. Ahn, R. M. Kasi, S. C. Kim, N. Sharma and Y. X. Zhou, *Soft Matter*, 2008, **4**, 1151–1157.
2 J. F. Mano, *Adv. Eng. Mater.*, 2008, **10**, 515–527.
3 P. M. Mendes, *Chem. Soc. Rev.*, 2008, **37**, 2512–2529.
4 I. Tokarev and S. Minko, *Soft Matter*, 2009, **5**, 511–524.
5 I. Tokarev and S. Minko, *Adv. Mater.*, 2009, **21**, 241–247.
6 J. L. Zhang and Y. C. Han, *Chem. Soc. Rev.*, 2010, **39**, 676–693.
7 M. Berggren and A. Richter-Dahlfors, *Adv. Mater.*, 2007, **19**, 3201–3213.
8 G. Decher, *Science*, 1997, **277**, 1232–1237.
9 G. Decher, J. D. Hong and J. Schmitt, *Thin Solid Films*, 1992, **210–211**, 831–835.
10 P. T. Hammond, *Adv. Mater.*, 2004, **16**, 1271–1293.
11 J. L. Lutkenhaus and P. T. Hammond, *Soft Matter*, 2007, **3**, 804–816.
12 D. M. Lynn, *Adv. Mater.*, 2007, **19**, 4118–4130.
13 S. A. Sukhishvili, *Curr. Opin. Colloid Interface Sci.*, 2005, **10**, 37–44.
14 F. Boulmedais, C. S. Tang, B. Keller and J. Vörös, *Adv. Funct. Mater.*, 2006, **16**, 63–70.
15 L. Dieguez, N. Darwish, N. Graf, J. Vörös and T. Zambelli, *Soft Matter*, 2009, **5**, 2415–2421.
16 O. Guillaume-Gentil, N. Graf, F. Boulmedais, P. Schaaf, J. Vörös and T. Zambelli, *Soft Matter*, 2010, **6**, 4246–4254.
17 F. Wang, D. Li, G. P. Li, X. Q. Liu and S. J. Dong, *Biomacromolecules*, 2008, **9**, 2645–2652.
18 K. C. Wood, N. S. Zacharia, D. J. Schmidt, S. N. Wrightman, B. J. Andaya and P. T. Hammond, *Proc. Natl. Acad. Sci. U. S. A.*, 2008, **105**, 2280–2285.
19 E. S. Forzani, M. A. Perez, M. L. Teijelo and E. J. Calvo, *Langmuir*, 2002, **18**, 9867–9873.
20 D. Grieshaber, J. Vörös, T. Zambelli, V. Ball, P. Schaaf, J. C. Voegel and F. Boulmedais, *Langmuir*, 2008, **24**, 13668–13676.
21 D. J. Schmidt, F. Ç. Cebeci, Z. I. Kalcioglu, S. G. Wyman, C. Ortiz, K. J. Van Vliet and P. T. Hammond, *ACS Nano*, 2009, **3**, 2207–2216.
22 R. Zahn, J. Vörös and T. Zambelli, *Curr. Opin. Colloid Interface Sci.*, 2010, **15**, 427–434.

23 D. M. DeLongchamp and P. T. Hammond, *Adv. Funct. Mater.*, 2004, **14**, 224–232.
24 D. J. Schmidt and P. T. Hammond, *Chem. Commun.*, 2010, **46**, 7358–7360.
25 I. C. Kwon, Y. H. Bae and S. W. Kim, *Nature*, 1991, **354**, 291–293.
26 T. K. Tam, M. Pita, M. Motornov, I. Tokarev, S. Minko and E. Katz, *Adv. Mater.*, 2010, **22**, 1863.
27 T. K. Tam, M. Pita, O. Trotsenko, M. Motornov, I. Tokarev, J. Halamek, S. Minko and E. Katz, *Langmuir*, 2010, **26**, 4506–4513.
28 J. Hiller and M. F. Rubner, *Macromolecules*, 2003, **36**, 4078–4083.
29 K. Itano, J. Y. Choi and M. F. Rubner, *Macromolecules*, 2005, **38**, 3450–3460.
30 D. Lee, A. J. Nolte, A. L. Kunz, M. F. Rubner and R. E. Cohen, *J. Am. Chem. Soc.*, 2006, **128**, 8521–8529.
31 O. Guillaume-Gentil, R. Zahn, S. Lindhoud, N. Graf, J. Vörös and T. Zambelli, *Soft Matter*, 2011, **7**, 3861–3871.
32 J. Choi and M. F. Rubner, *Macromolecules*, 2005, **38**, 116–124.
33 C. Deslouis, I. Frateur, G. Maurin and B. Tribollet, *J. Appl. Electrochem.*, 1997, **27**, 482–492.
34 G. E. Zaikov, A. L. Iordanskii and V. S. Markin, *Diffusion of Electrolytes in Polymers*, VSP, Utrecht, Netherlands, 1988.
35 A. L. Smith, J. N. Ashcraft and P. T. Hammond, *Thermochim. Acta*, 2006, **450**, 118–125.
36 J. W. Yoon, S. Q. Cai, Z. G. Suo and R. C. Hayward, *Soft Matter*, 2010, **6**, 6004–6012.
37 D. Johannsmann, *Phys. Chem. Chem. Phys.*, 2008, **10**, 4516–4534.
38 M. V. Voinova, M. Rodahl, M. Jonson and B. Kasemo, *Phys. Scr.*, 1999, **59**, 391–396.
39 J. Cho, K. Char, J. D. Hong and K. B. Lee, *Adv. Mater.*, 2001, **13**, 1076–1078.
40 B. D. Vogt, E. K. Lin, W. L. Wu and C. C. White, *J. Phys. Chem. B*, 2004, **108**, 12685–12690.
41 L. E. Nielsen and R. F. Landel, *Mechanical Properties of Polymers and Composite*, Marcel Dekker, New York, 1994.
42 B. Oommen and K. J. Van Vliet, *Thin Solid Films*, 2006, **513**, 235–242.
43 G. Francius, J. Hemmerle, V. Ball, P. Lavalle, C. Picart, J. C. Voegel, P. Schaaf and B. Senger, *J. Phys. Chem. C*, 2007, **111**, 8299–8306.
44 E. K. Dimitriadis, F. Horkay, J. Maresca, B. Kachar and R. S. Chadwick, *Biophys. J.*, 2002, **82**, 2798–2810.
45 M. Bahrami-Samani, C. D. Cook, J. D. Madden, G. M. Spinks and P. G. Whitten, *Thin Solid Films*, 2008, **516**, 2800–2807.
46 C. Barbero and R. Kotz, *J. Electrochem. Soc.*, 1994, **141**, 859–865.
47 L. Lizarraga, E. M. Andrade and F. V. Molina, *J. Electroanal. Chem.*, 2004, **561**, 127–135.
48 M. A. Mohamoud and A. R. Hillman, *Electrochim. Acta*, 2007, **53**, 1206–1216.
49 R. Z. Pytel, E. L. Thomas and I. W. Hunter, *Polymer*, 2008, **49**, 2008–2013.
50 P. R. Singh, S. Mahajan, S. Raiwadec and A. Q. Contractor, *J. Electroanal. Chem.*, 2009, **625**, 16–26.
51 E. Smela and N. Gadegaard, *J. Phys. Chem. B*, 2001, **105**, 9395–9405.